Quantum signature of the classical chaos in the field-induced barrier crossing in a quartic potential*

P. K. Chattaraj†, S. Sengupta and A. Poddar

Department of Chemistry, Indian Institute of Technology, Kharagpur 721 302, India

The quantum domain behaviour of a classical double-well oscillator which exhibits chaos in the presence of an external monochromatic field has been studied using Bohmian mechanics. The classical Kolmogorov–Arnol'd–Moser (KAM) tori break down in the presence of an external perturbation for which the corresponding quantal phase portrait exhibits regular islands owing to the quantum suppression of the classical chaos. It has also been observed that the classical chaos generally enhances the quantum fluctuations.

THERE has been a recent upsurge of interest in the study of the quantum dynamics of classically chaotic systems[1–14]. It has been shown[1–14] that the quantum nonclassical effects suppress the classical stochasticity. An integrable classical system or a system in the presence of a weak perturbation is characterized by invariant KAM tori. The phase space begins to appear chaotic when the amplitude of the external destabilizing field is increased[15]. The KAM tori in this case break down into cantori[16] which help in stabilizing the corresponding quantum system[13,14]. In order to understand these aspects better we study the quantum domain behaviour of a quartic oscillator in the presence of an external monochromatic field. This problem is considered to be important in several areas of chemical dynamics[17] and has been studied in detail[13–15] in recent years. It has been observed[13,14] that the classical chaos and quantum tunneling occur simultaneously in this case to give rise to the coherent oscillatory nature of the quantum diffusion between two stable KAM tori.

Quantum potential based approaches[1,18–20] offer a good quantum description of classically chaotic systems. In quantum fluid dynamics (QFD)[18], the overall motion of the system is mapped onto the motion of a 'probability fluid' having density $\rho(\mathbf{r}, t)$ and velocity $v(\mathbf{r}, t)$ under the influence of the external classical potential augmented by a quantum potential. The basic equations of QFD comprise an equation of continuity and an Euler-type equation of motion. It has been shown[9] that these equations can be written in the form of Hamilton's equations of motion with a Hamiltonian functional properly defined for this purpose and by considering $\rho(\mathbf{r}, t)$ and $(-\chi(\mathbf{r}, t))$ as canonically conjugate variables, where $\chi(\mathbf{r}, t)$ is the velocity potential. Chaotic dynamics of a quantum Hénon-Heiles oscillator has been studied[9] using QFD, in terms of ρ versus $(-\chi)$ plots and time evolution of several time-dependent density functionals like Shannon entropy, density correlation and macroscopic kinetic energy. Another quantum potential-based theory is the quantum theory of motion (QTM)[1] in the sense of classical interpretation of quantum mechanics as developed by de Broglie[19] and Bohm[20]. In QTM[1], the overall motion of a physical system is understood in terms of both wave and particle pictures. The pertinent time-dependent Schrödinger equation (TDSE) governs the wave motion. This wave guides a point particle whose motion is described in terms of forces originating from the classical as well as quantum potentials. In QTM, important insights into quantum domain chaotic dynamics are obtained[10,11] in terms of the phase space distance between two initially close Bohmian trajectories and the associated Kolmogorov–Sinai (KS) entropy. Quantum standard map[11], Weigert's quantum cat map[11], Rydberg atoms in external fields[10] and a quantum Hénon-Heiles oscillator[10] have been studied successfully using QTM. Possibility of a QTM for many-electron systems is being explored[21] within a quantum fluid density functional framework[22].

In the present work, we apply QTM in analysing the quantum analogue of the classical domain chaotic dynamics associated with the penetration of a barrier in a double-well potential in the presence of a monochromatic external field with increasing amplitude.

The classical Hamiltonian of a double-well oscillator under the influence of an external oscillating driving force is given by:

$$\mathcal{H} = \frac{p^2}{2m} + ax^4 - bx^2 + c\cos(\omega_0 t). \tag{1}$$

For a given set of parameter values, the classical Hamilton's equations of motion can be solved[13,14] to generate the stroboscopic plots of various trajectories. Depending on the choice of the initial position and momentum values one may obtain stable regions in phase space bounded by KAM surfaces or a chaotic sea extended over the whole phase space.

In order to get a quantum mechanical description of this problem, the classical Hamiltonian (eq. (1)) is directly quantized and the pertinent TDSE has been written as:

$$\hat{\mathcal{H}}\psi(x,t) = \left[-\frac{1}{2}\frac{d^2}{dx^2} + ax^4 - bx^2 + c\cos(\omega_0 t)\right]\psi(x,t)$$

$$= i\frac{\partial\psi(x,t)}{\partial t}. \tag{2}$$

*This paper is based on a seminar talk delivered by P. K. Chattaraj at the International Conference on Nonlinear Dynamics: Integrability and Chaos, at the Centre for Nonlinear Dynamics, Bharathidasan University, Tiruchirapalli in February 1998.

†For correspondence. (email: pkcj@hijli.iitkgp.ernet.in)

Atomic units are used throughout unless otherwise specified. The complete description of a physical system involves both wave and particle pictures in QTM[1]. While the wave motion is governed by the TDSE, the motion of a point particle guided by this wave is characterized by its velocity as given by:

$$\dot{x} = \nabla\chi(x,t)|_{x=x(t)}, \tag{3}$$

where χ is the velocity potential expressed as the phase of the wavefunction in its polar form as follows:

$$\psi(x, t) = \rho^{1/2}(x, t) \exp[i\chi(x, t)]. \tag{4}$$

An assembly of initial positions will constitute an ensemble of particle motions guided by the same wave, and the probability that the particle be present between x and $x + dx$ in this ensemble at time t is given by[1] $\rho(x, t)dx$. Solution of eq. (3) with various initial positions would yield the so-called 'Bohmian trajectories'. A phase space distance function can be defined as follows[10,11] in order to study the quantum signature of chaos through sensitive dependence on initial conditions,

$$D(t) = \{(x_1(t) - x_2(t))^2 + (p_{x_1}(t) - p_{x_2}(t))^2\}^{1/2}, \tag{5}$$

where (x, p_x) refers to a point in phase space.

A generalized quantum Lyapunov exponent has also been defined as[11]:

$$\Lambda = \lim_{\substack{D(t)\to 0 \\ t\to\infty}} \frac{1}{t} \ln\left[\frac{D(t)}{D(0)}\right]. \tag{6}$$

The corresponding KS entropy is given by[11]:

$$H = \sum_{\Lambda_+ > 0} \Lambda_+ . \tag{7}$$

Chaotic quantum dynamics is characterized by a positive KS entropy[11].

The phase space volume is defined as[12]:

$$V_{ps}(t) = [\langle (x - \langle x\rangle)^2\rangle \langle (p_x - \langle p_x\rangle)^2\rangle]^{1/2}. \tag{8}$$

A sharp increase in $V_{ps}(t)$ implies a chaotic motion[10,12]. This quantity is same as the associated uncertainty product which can be used as a measure of quantum fluctuations[14]. Classical chaos generally enhances quantum fluctuations[10,12,14].

The double-well potential used in the present problem is given by:

$$V(x) = ax^4 - bx^2 + c\cos(\omega_0 t), \tag{9}$$

where the parameter values are taken as follows[13]: $a = 0.5$, $b = 10.0$, $c = 10.0$ and $\omega_0 = 6.07$. Classical phase-portraits and their QTM counterparts are generated for two different initial conditions, $(x, p_x)|_{t=0}$, viz. (a) (–2.0, 0.0) and (b) (2.0, 0.0). For the given set of parameter values the classical motion is regular for case (a) and chaotic for case (b) although both the cases correspond to the same value of the unperturbed energies of the double-well oscillator.

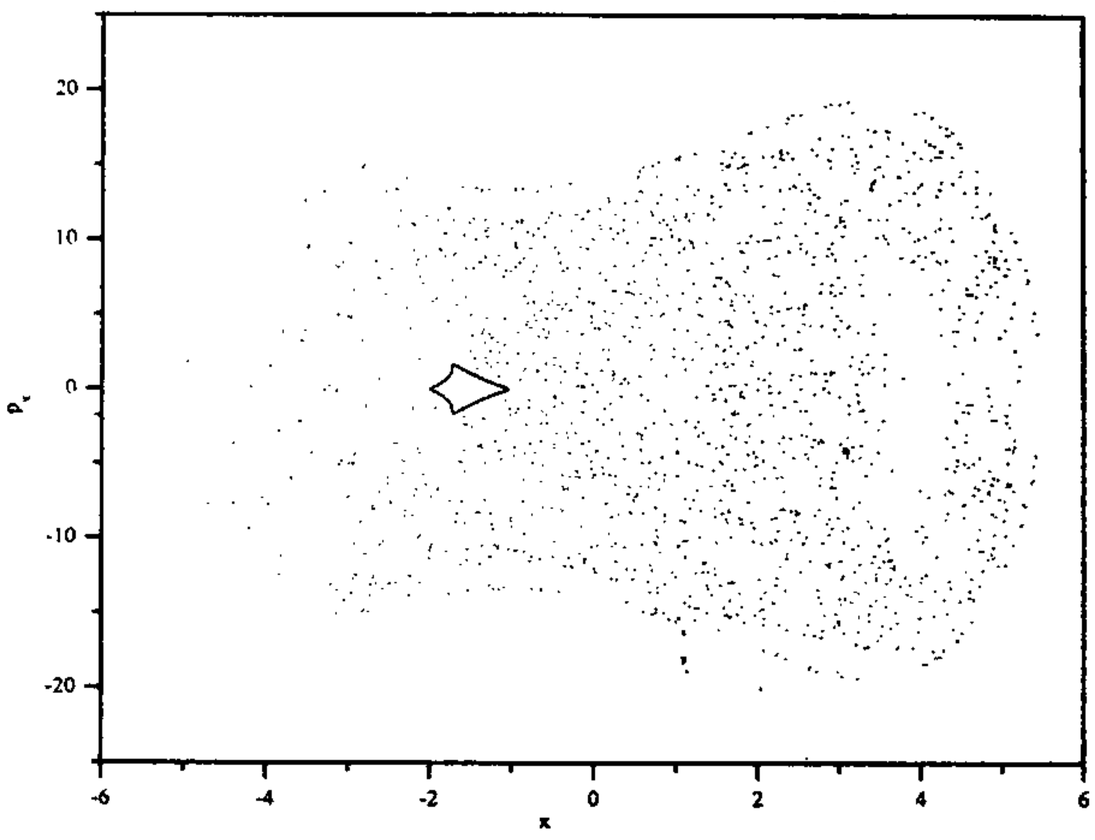

Figure 1. Classical phase space trajectories for a double-well oscillator in the presence of an external field with $c = 10$ and two different initial conditions: (a) $(x_0 = -2.0,\ p_0 = 0.0)$; (b) $(x_0 = 2.0,\ p_0 = 0.0)$.

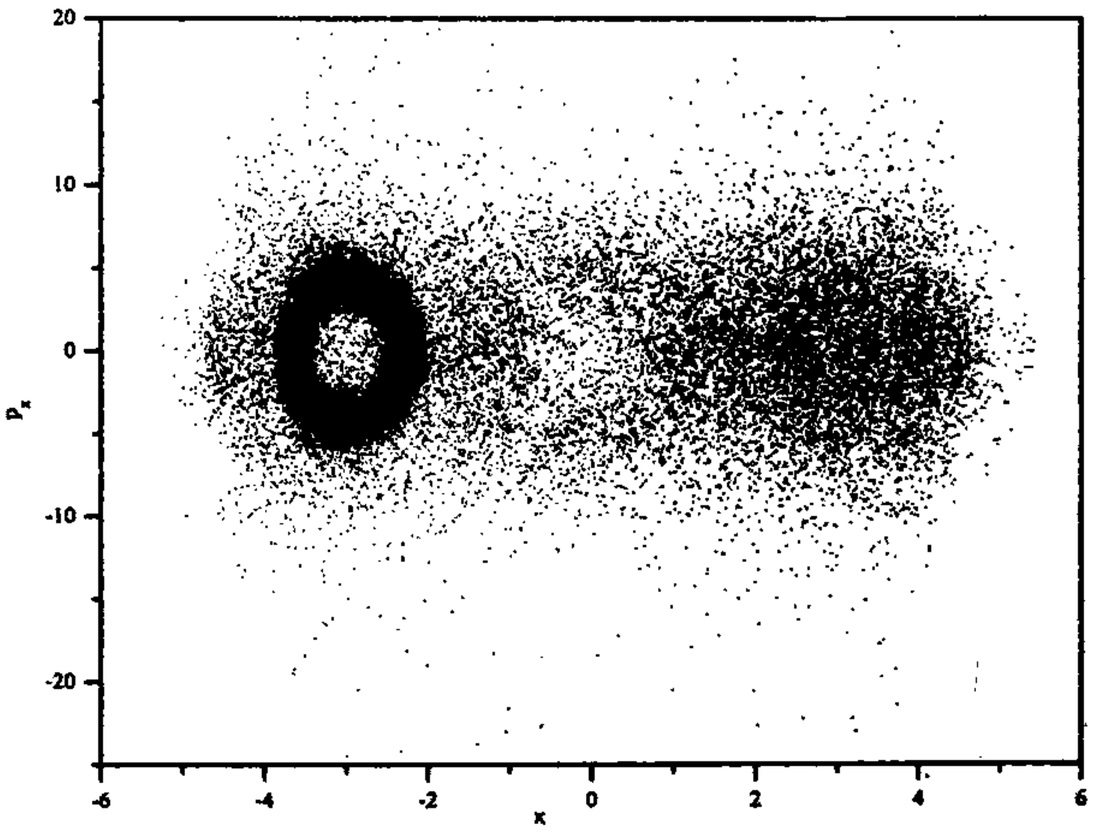

Figure 2. Quantal phase space trajectories for a double-well oscillator in the presence of an external field with $c = 10$ and two different initial conditions: (a) $(x_0 = -2.0,\ p_0 = 0.0)$; (b) $(x_0 = 2.0,\ p_0 = 0.0)$.

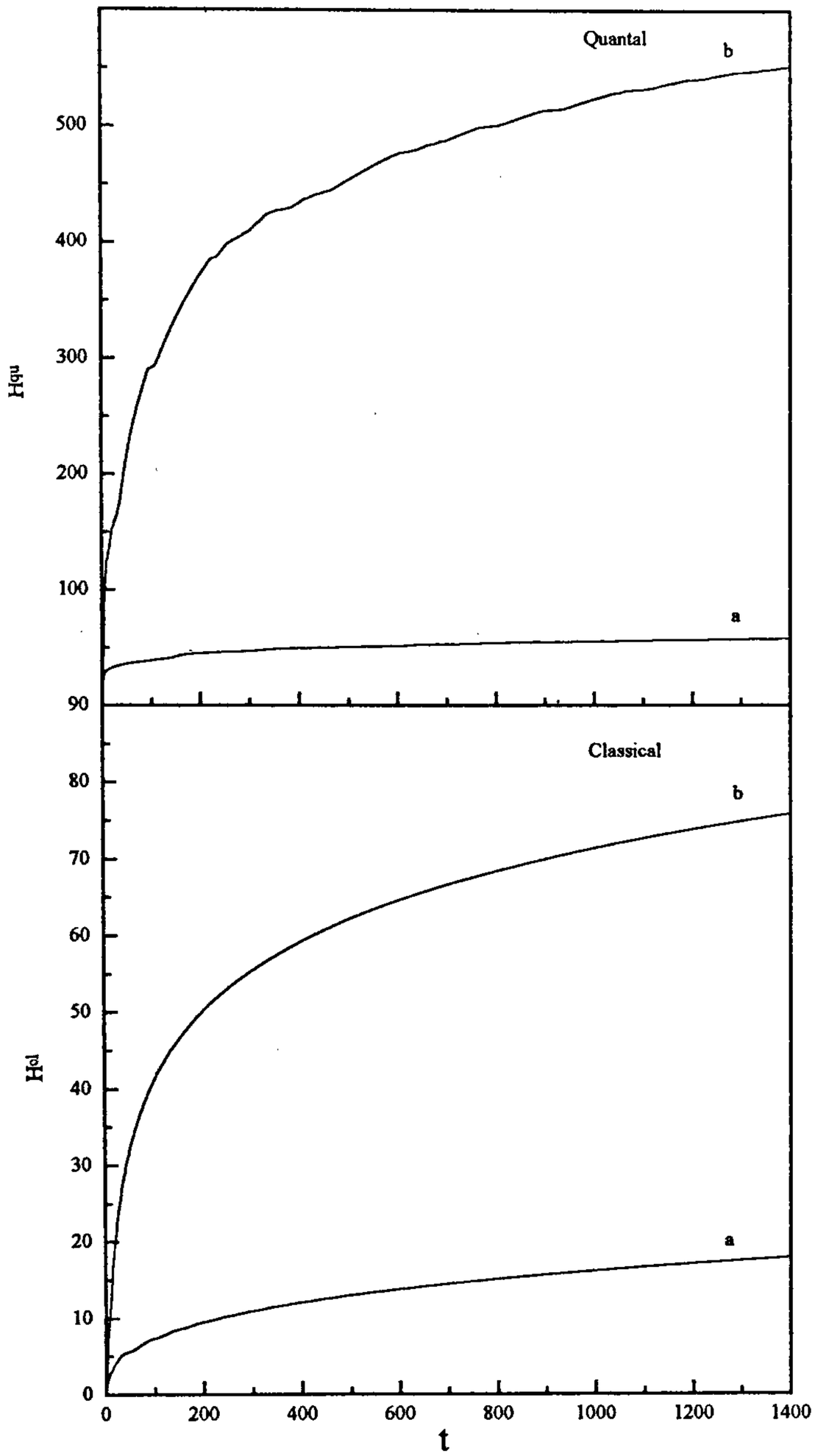

Figure 3. Time evolution of the KS entropy associated with the classical motion (H^{cl}) and quantal motion (H^{qu}) for a double-well oscillator in the presence of an external field with $c = 10$ and two different initial conditions: (a) ($x_0 = -2.0$, $p_0 = 0.0$); (b) ($x_0 = 2.0$, $p_0 = 0.0$).

To understand the classical regular/chaotic motion associated with the field-induced barrier penetration in a quartic potential we solve the relevant classical Hamilton's equations of motion using a fourth order Runge–Kutta method. In order to study the corresponding quantum signatures we generate the respective Bohmian trajectories. For this purpose, the numerical solution is launched with the propagation of a Gaussian wavepacket under the influence of the quartic potential (eq. (9)). The details of the numerical solution are available elsewhere[10,23]. Mesh sizes adopted are $\Delta x = 0.1$ and $\Delta t = 0.02$. Calculation is carried out for $-15 \leq x \leq 15$ and for 10^5 time-steps. It may be noted that the classical phase space

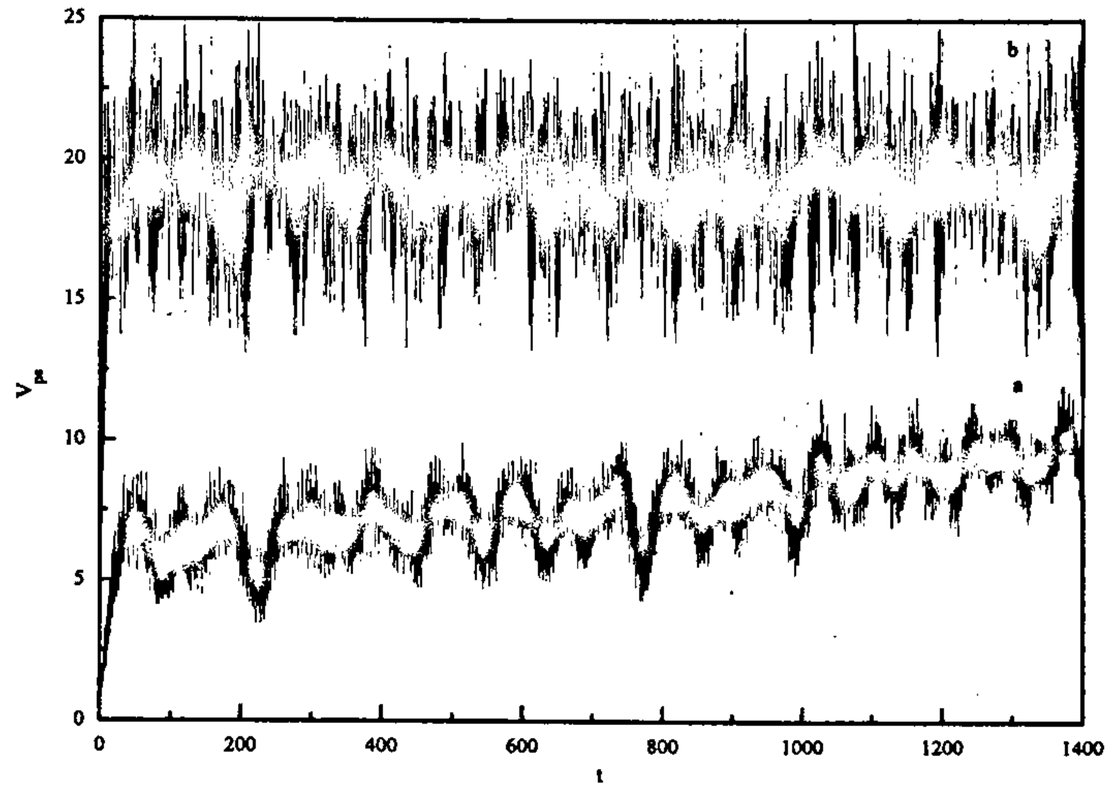

Figure 4. Time evolution of the phase space volume V_{ps} associated with the quantal motion for a double-well oscillator in the presence of an external field with $c = 10$ and two different initial conditions: (a) ($x_0 = -2.0$, $p_0 = 0.0$); (b) ($x_0 = 2.0$, $p_0 = 0.0$).

for this problem is three-dimensional (x, p, t) and hence possesses the minimum number of phase space degrees of freedom to exhibit the possible chaotic behaviour. However, momentum is not a 'true variable' in the case of the corresponding quantum system. In the present study, like others[9–14], we are interested in the signature of the classically chaotic motion, if any, in the associated quantum dynamics.

Once we know $\psi(x, t)$, we can rewrite eq. (3) as:

$$\dot{\mathbf{x}} = \nabla\chi(x,t)|_{x=x(t)} = \mathrm{Re}\left[-\frac{i\nabla\psi}{\psi}\right], \tag{10}$$

which has been solved with two different initial conditions (cases (a) and (b)) to obtain the Bohmian trajectories. A second-order Runge–Kutta method is used for this purpose.

In order to understand the breakdown[15] of KAM tori with increasing amplitude of the external field and a possible quantum suppression of the classical chaos, the calulation for case (a) is repeated for two other values of c, viz. 20, 40.

Figure 1 depicts the classical phase space trajectories (stroboscopic plots) for the double-well oscillator in the presence of an external field for two different initial conditions (cases (a) and (b)). While case (a) corresponds to a regular island, case (b) gives rise to the chaotic sea. The KAM torus is surrounded by the following phase-space points, (x, p_x), in this case: (−2.00, 0.00), (−1.05, 0.00), (−1.72, −1.65) and (−1.72, 1.65).

Corresponding quantal phase portraits generated through the respective Bohmian trajectories are presented in Figure 2. The quantal behaviour properly mimicks the underlying classical dynamics, viz. a regular island for case (a) and a chaotic sea for case (b). It

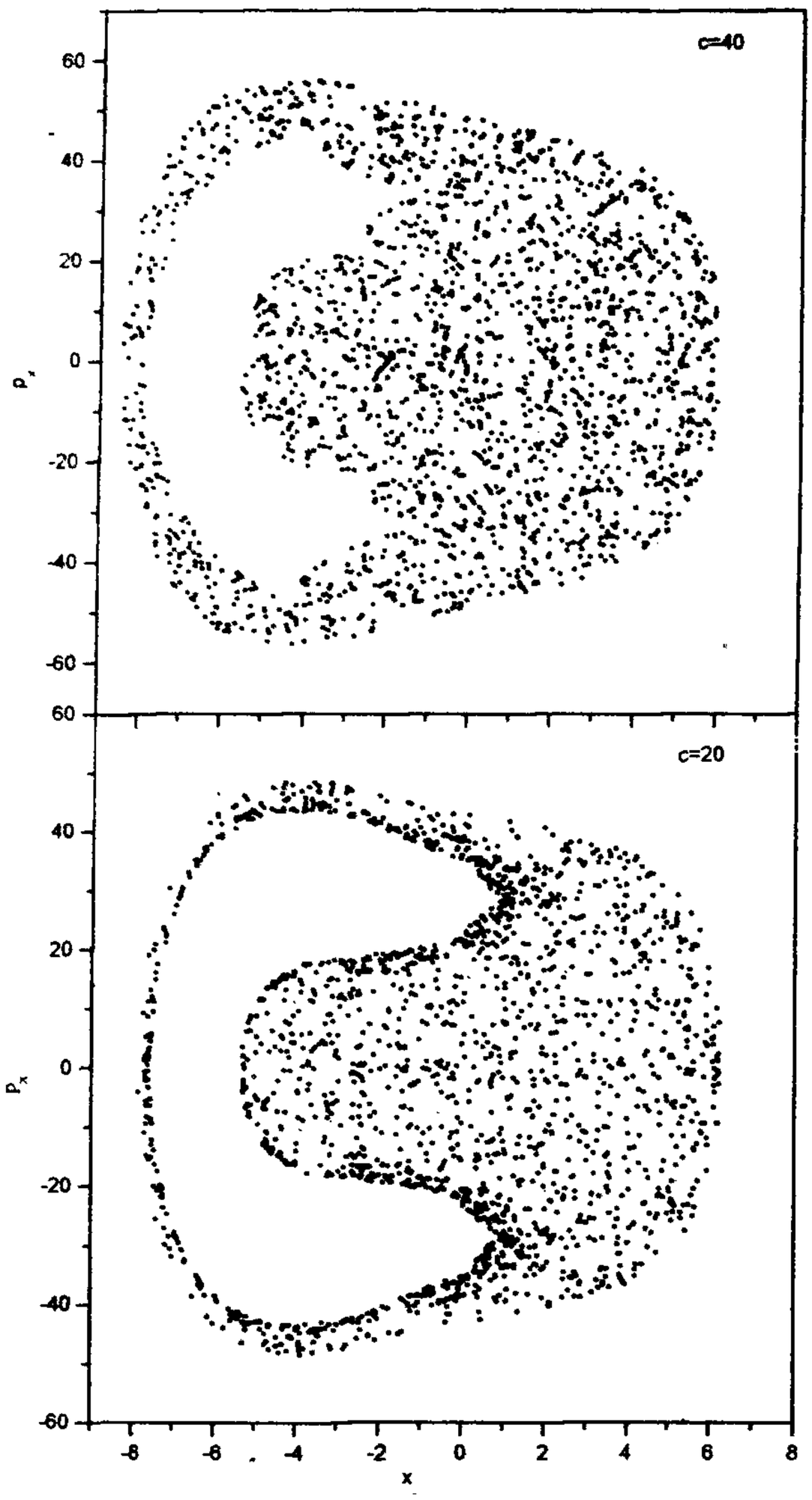

Figure 5. Classical phase space trajectory for a double-well oscillator in the presence of an external field with $c = 20$ and $c = 40$ with initial condition: ($x_0 = -2.0$, $p_0 = 0.0$).

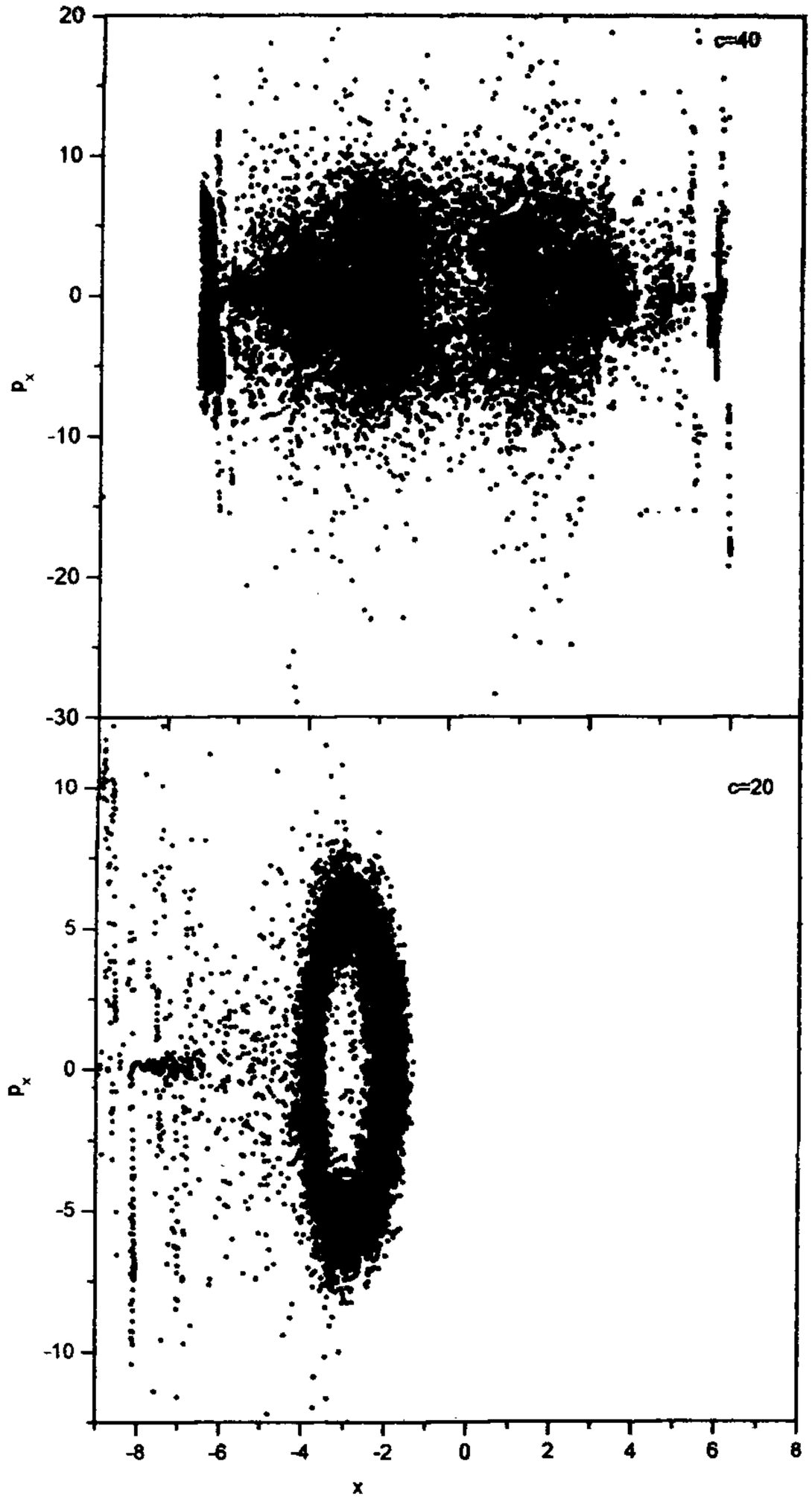

Figure 6. Quantal phase space trajectory for a double-well oscillator in the presence of an external field with $c = 20$ and $c = 40$ with initial condition: ($x_0 = -2.0$, $p_0 = 0.0$).

appears that a cantorus-like structure[16] is a quantum equivalent of the classical KAM torus. The cantorus is 'bounded' by the following phase-space points: (–3.90, 0.00), (–2.00, 0.00), (–3.00, 5.00) and (–3.00, –5.00). It is important to note that although the initial conditions associated with classical regular/chaotic behaviour give rise to quantal regular/chaotic behaviour, the size and the position of the classical KAM torus are not necessarily the same as those of the quantal cantorus.

Figures 3 and 4 present respectively the classical (H^{cl}) and quantal (H^{qu}) KS entropies and the phase space volume (V_{ps}). It may be noted that the orders of magnitude of H^{cl} and H^{qu} are not the same. It is, however, transparent in these plots that the classical stochasticity enhances quantal fluctuations.

In order to investigate the breakdown of the KAM torus[15] (case (a)) when the strength of the perturbation is increased as well as any possible quantum suppression[1–14] of the classical chaos, we study the behaviour of the double-well oscillator in the presence of the external field with two other amplitudes, viz. $c = 20$ and 40, and the same initial conditions as in case (a) which corresponds to a regular motion for $c = 10$.

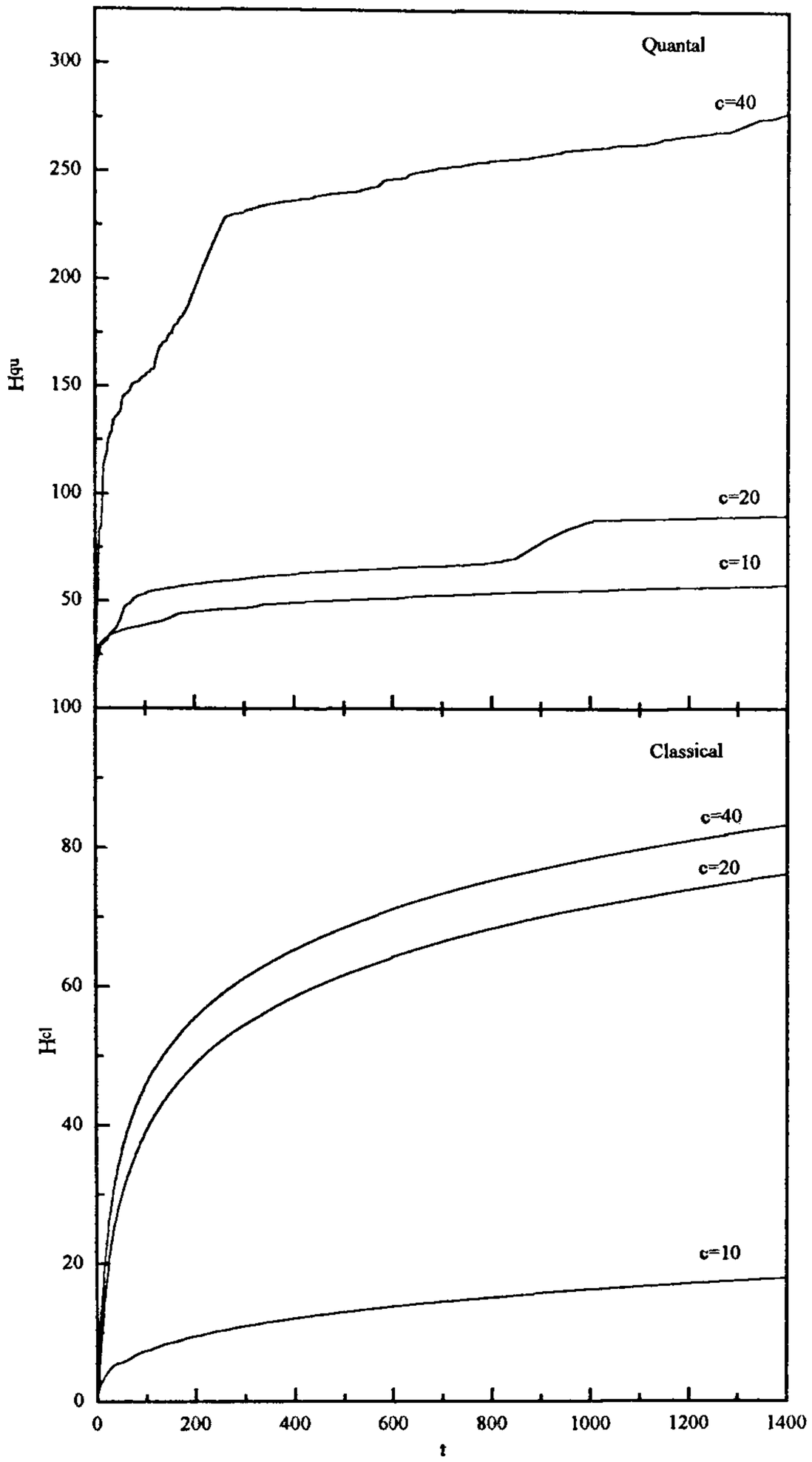

Figure 7. Time evolution of the KS entropy associated with the classical motion (H^{cl}) and quantal motion (H^{qu}) for a double-well oscillator in the presence of an external field with $c = 10$, 20 and 40 respectively, with initial condition: ($x_0 = -2.0$, $p_0 = 0.0$).

Figure 5 presents the stroboscopic plots of the classical trajectories for case (a) corresponding to $c = 20$ and $c = 40$, respectively. It is transparent in these plots that the regular island ($c = 10$) is destroyed and the phase space appears to be completely chaotic, more pronounced for the higher c value. Similar plots for the respective quantal motion are given in Figure 6. It is quite clear that a 'cantorus-like' island still persists for $c = 20$ which, however, breaks down for $c = 40$. This fact provides an unmistakable signature of the quantum suppression of chaos. The size and the position of the

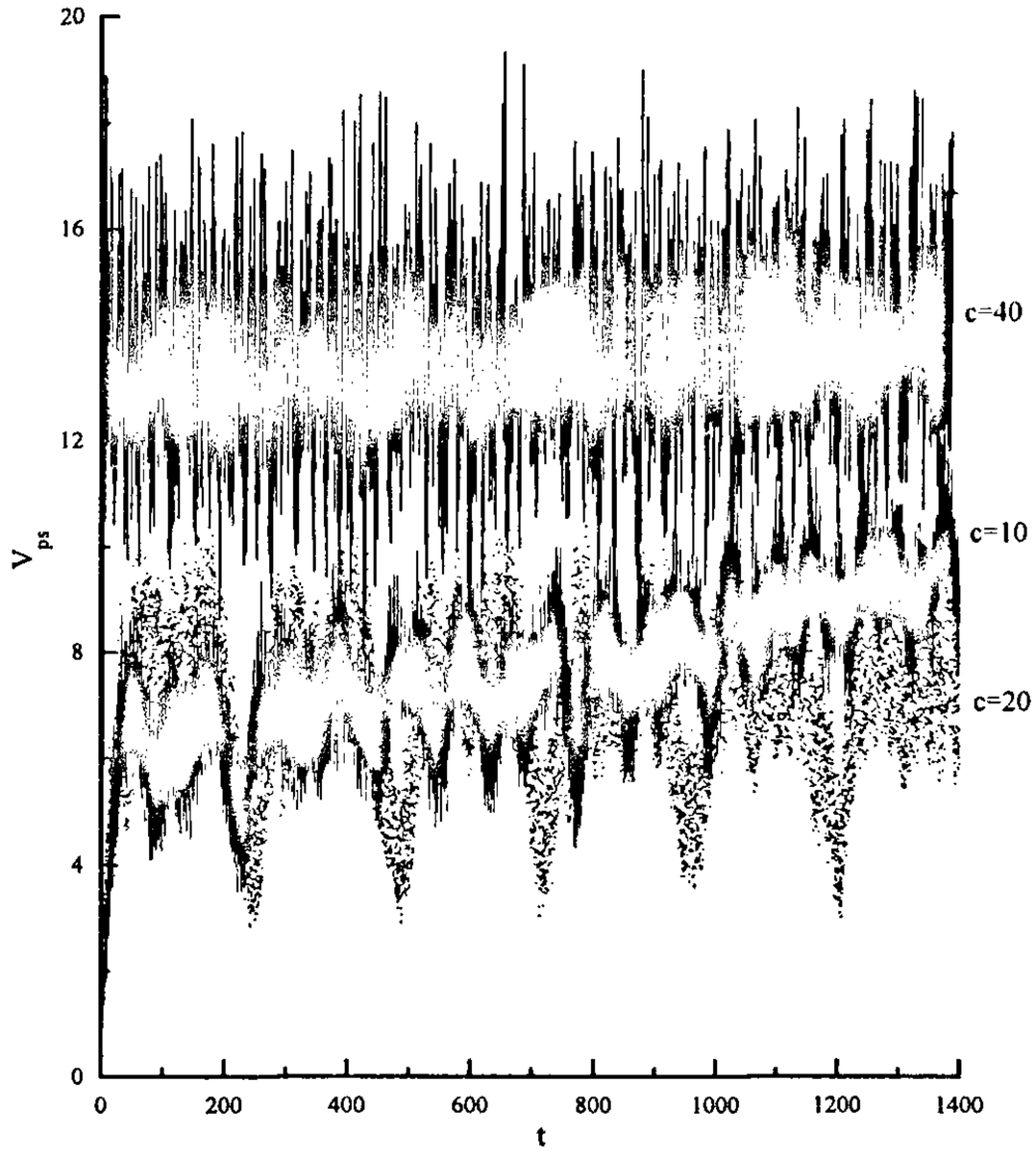

Figure 8. Time evolution of the phase space volume V_{ps} associated with the quantal motion for a double-well oscillator in the presence of an external field with $c = 10$, 20 and 40 respectively, with initial condition: ($x_0 = -2.0$, $p_0 = 0.0$).

cantorus ($c = 20$) remain more or less the same as in the case of $c = 10$.

Figure 7 depicts H^{cl} and H^{qu} while Figure 8 presents V_{ps} for the above mentioned cases. These quantities mimick all the trends and strengthen the above inference. For the classical case, H^{cl} remains small for $c = 10$ but increases rapidly for the other two c values. For $c = 10$ and 20, H^{qu} values are relatively much smaller when compared to the corresponding value for $c = 40$. When the cantorus breaks down ($c = 40$), very large quantum fluctuations are clearly revealed by the V_{ps} plots while the V_{ps} values are comparable for $c = 10$ and 20.

To summarize, important insights into the quantum manifestations of the classical regular and chaotic motions of a double-well oscillator in the presence of an external field with different amplitudes have been obtained in terms of the corresponding Bohmian trajectories. Two quantum systems which exhibit regular and chaotic motions respectively in the classical domain can be differentiated with the help of the quantum theory of motion. It has been demonstrated for the first time in terms of stroboscopic plots within a Bohmian mechanical framework that the classical chaos enhances the quantum fluctuations and quantum nonclassical effects suppress the classical stochasticity. The KS entropy and phase space volume support this result.

1. Holland, P. R., in *The Quantum Theory of Motion*, Cambridge University Press, Cambridge, 1993.
2. Gutzwiller, M. C., in *Chaos in Classical and Quantum Mechanics*, Springer, Berlin, 1990.
3. Eckhardt, B., *Phys. Rep.*, 1988, **163**, 205–209.
4. Jensen, R. V., *Nature*, 1992, **355**, 311–317; *ibid*, 1995, **373**, 16.
5. Casati, G., Chirikov, B. V., Shepelyansky, D. L. and Guarneri, I., *Phys. Rev. Lett.*, 1986, **57**, 823–826; Casati, G., Chirikov, B. V., Guarneri, I. and Shepelyansky, D. L., *Phys. Rep.*, 1987, **154**, 77–123; Casati, G., Chirikov, B. V., Izrailev, F. M. and Ford, J., in *Stochastic Behaviour in Classical and Quantum Hamiltonian Systems* (eds Casati, G. and Ford, J.), Springer, Berlin, 1979.
6. de Polavieja, G. G., *Phys. Rev. A*, 1996, **53**, 2059–2061; *Phys. Lett. A*, 1996, **220**, 303. Frisk, H., *Phys. Lett. A*, 1997, **227**, 139; Konkel, S. and Makowski, A. J., *Phys. Lett. A*, 1998, **238**, 95–100.
7. Berry, M. V. and Balazs, N. L., *J. Phys. A*, 1979, **12**, 625–642; Hogg, T. and Huberman, B. A., *Phys. Rev. Lett.*, 1982, **48**, 711; Grempel, D. R., Fishman, S. and Prange, R. E., *Phys. Rev. Lett.*, 1984, **53**, 1212–1216; Chang, S. and Shi, K., *Phys. Rev. Lett.*, 1985, **55**, 269–272.
8. Nakamura, K. and Lakshmanan, M., *Phys. Rev. Lett.*, 1986, **57**, 1661–1664; Nakamura, K. and Thomas, H., *Phys. Rev. Lett.*, 1988, **61**, 247–250; Nakamura, K. and Mikeska, H. J., *Phys. Rev. A*, 1987, **35**, 5294–5297; Nakamura, K., Bishop, A. R. and Shudo, A., *Phys. Rev. B*, 1989, **39**, 12422–12425.
9. Chattaraj, P. K. and Sengupta, S., *Phys. Lett. A*, 1993, **181**, 225–231; Chattaraj, P. K., *Indian J. Pure Appl. Phys.*, 1994, **32**, 101–105; Chattaraj, P. K. and Sengupta, S., *Indian J. Pure Appl. Phys.*, 1996, **34**, 518–527.
10. Sengupta, S. and Chattaraj, P. K., *Phys. Lett. A*, 1996, **215**, 119–127; Chattaraj, P. K. and Sengupta, S., *Curr. Sci.*, 1996, **71**, 134–139; Chattaraj, P. K., Sengupta, S. and Poddar, A., *Curr. Sci.*, 1998, **74**, 758–764.
11. Schwengelbeck, U. and Faisal, F. H. M., *Phys. Lett. A*, 1995, **199**, 281–286; Faisal, F. H. M. and Schwengelbeck, U., *Phys. Lett. A*, 1995, **207**, 31–36.
12. Feit, M. D. and Fleck, Jr. J. A., *J. Chem. Phys.*, 1984, **80**, 2578–2584.
13. Lin, W. A. and Ballentine, L. E., *Phys. Rev. Lett.*, 1990, **65**, 2927–2928.
14. Graham, R. and Hohnerbach, H., *Phys. Rev. A*, 1991, **43**, 3966–3981; *Phys. Rev. Lett.*, 1990, **64**, 637–640; Chaudhuri, S., Gangopadhyay, G. and Ray, D. S., *Indian J. Phys. B*, 1995, **69**, 507–523.
15. Reichl, L. E. and Zhang, W. M., *Phys. Rev. A*, 1984, **29**, 2186–2193.
16. McKay, R. S. and Meiss, J. D., *Phys. Rev. A*, 1988, **37**, 4702–4706; Hanson, J. D., Cary, J. R. and Meiss, J. D., *J. Stat. Phys.*, 1985, **39**, 327–345; Meiss, J. D., *Parti. Accel.*, 1986, **19**, 9.
17. Hanggi, P., in *Activated Barrier Crossing* (eds Fleming, G. R. and Hanggi, P.), World Scientific, Singapore, 1993.
18. Madelung, E., *Z. Phys.*, 1926, **40**, 322–326; Deb, B. M. and Ghosh, S. K., *J. Chem. Phys.*, 1982, **77**, 342–348; Bartolotti, L. J., *Phys. Rev. A*, 1982, **26**, 2243–2244.
19. de Broglie, L., *C.R. Acad. Sci.*, 1926, **183**, 447–448; *ibid*, 1927, **184**, 273–274; *ibid*, 1927, **185**, 380–382.
20. Bohm, D., *Phys. Rev.*, 1952, **85**, 166–179, 180-193; in *Causality and Chance in Modern Physics*, Rouletge and Keegan Paul, London, 1957.
21. Chattaraj, P. K., Sengupta, S. and Poddar, A., *Int. J. Quantum Chem., DFT Special Issue*, 1998, **69**, 279–291; in *Nonlinear Dynamics and Computational Physics* (ed. Sheory, V. B.), Narosa, New Delhi, 1999, pp. 45–53.
22. Deb, B. M. and Chattaraj, P. K., *Phys. Rev. A*, 1989, **39**, 1696–1712.
23. Goldberg, A., Schey, H. M. and Schwartz, J. L., *Am. J. Phys.*, 1967, **35**, 177–186; *ibid*, 1968, **36**, 454–455; Galbraith, I., Ching, Y. S. and Abraham, E., *Am. J. Phys.*, 1984, **52**, 60–68.

ACKNOWLEDGEMENT. This article is dedicated to Prof. M. Lakshmanan on his 50th birthday. We thank CSIR, New Delhi for financial assistance. We are grateful to the referee for constructive criticism.

Received 28 December 1998; revised accepted 10 March 1999

Multicomponent coordinated defence response of rice to *Rhizoctonia solani* causing sheath blight

S. Bera and R. P. Purkayastha

Department of Botany, University of Calcutta, Calcutta 700 019, India

An excellent multicomponent coordinated defence response of rice plants (cv. IET-2233) to fungal attack has been demonstrated and a plausible relationship among them has been proposed. Some selected defence components such as momilactone 'A' (a rice phytoalexin), β-1,3-glucanases and exo chitinases (both pathogenesis related (PR)-proteins) and an enzyme phenylalanine ammonia lyase (PAL) were employed as biochemical parameters for evaluating the degree of response of rice plants to *Rhizoctonia solani* Kühn, a fungus causing sheath blight disease. A systemic fungicide kitazin which reduced disease significantly also concomitantly activated biosynthesis of momilactone A, induced PR-proteins and increased PAL activity in rice. Treatment of rice leaf sheaths with a PR-protein inhibitor (kinetin + NAA) increased disease markedly but inhibited β-1,3-glucanases and exo-chitinase activities in treated plants. Similarly, amino oxyacetic acid (AOA), a PAL inhibitor also enhanced disease intensity and inhibited PAL activity in treated, inoculated plants. Results confirm the coordinated function of various defence components in rice following infection by *Rhizoctonia* and also after abiotic induction of resistance.

USUALLY a plant responds to a pathogen by mobilizing a complex network of active defence mechanisms. The success of the plant in warding-off the pathogenic attack depends upon the coordination among the different defence strategies and the rapidity of the response. It is generally believed that plants defend themselves against pathogenic fungi by producing fungitoxic substances such as phytoalexins, pathogenesis related (PR)-